MATHEMATICAL BIOSCIENCES
AND ENGINEERING
Volume **7**, Number **2**, April **2010**

doi:10.3934/mbe.2010.7.259

pp. **259–275**

SURFACE TENSION AND MODELING OF CELLULAR INTERCALATION DURING ZEBRAFISH GASTRULATION

Colette Calmelet

Department of Mathematics and Statistics, California State University
Holt Hall 181, Chico, CA 95929, USA

Diane Sepich

Department of Biological Sciences, Vanderbilt University
MRBIII Suite 4260A, Nashville, TN 37203, USA

(Communicated by James Glazier)

Abstract. In this paper we discuss a model of zebrafish embryo notochord development based on the effect of surface tension of cells at the boundaries. We study the process of interaction of mesodermal cells at the boundaries due to adhesion and cortical tension, resulting in cellular intercalation. From in vivo experiments, we obtain cell outlines of time-lapse images of cell movements during zebrafish embryo development. Using Cellular Potts Model, we calculate the total surface energy of the system of cells at different time intervals at cell contacts. We analyze the variations of total energy depending on nature of cell contacts. We demonstrate that our model can be viable by calculating the total surface energy value for experimentally observed configurations of cells and showing that in our model these configurations correspond to a decrease in total energy values in both two and three dimensions.

1. **Introduction.** In this paper we analyze a model of notochord development of the zebrafish embryo. Particularly, we are interested in studying factors contributing to the (mediolateral) intercalation of mesodermal cells. By intercalation we mean a reordering of the cells resulting in their elongation, alignment in certain (mediolateral) direction, their insertion in the spaces between other cells, along with subsequent formation of a column of cells leading to the zebrafish notochord development.

For the past few years a number of problems related to the modeling of the morphogenetic movements of different species have been discussed in the literature [2], [3], [6], [8], [9], [13], [14], [17], [18]. Here we mention two types of approaches to mathematical modeling of the process of intercalation. Most papers follow the simulation approach, which is based on assumed initial conditions and testing of chosen values of model parameters. The validity of this approach is verified by comparison with experimental data, which generally is not easy to do. In our approach we do not employ simulation; instead we calculate the total energy values for those configurations of cells that lead to cell intercalation and discuss the total energy variation depending on the values of model parameters. Some parameters

2000 *Mathematics Subject Classification.* Primary: 92-08, 92-C15; Secondary: 65C05, 68U99.
Key words and phrases. Cellular intercalation, Cellular Potts Model, zebrafish, surface tension, anisotropic adhesion, cortical tension, total energy, mophogenetic movements, modeling, stability.

are determined directly from existing experimental data (observation of notochord formation), and others remain unknown variables of the model. We test our model by showing a decrease in time of the total surface energy values for configurations observed in the experiment.

For our analysis we utilize in vivo experimental data showing subsequent changes in the cell boundary outlines with time. We will show that the process of cell intercalation described by our model is stable in a sense that the total surface energy of the system decreases with time. According to the model, the total surface tension energy of the system of cells is determined as the sum of cell adhesion and cortical tension energies at the cell boundary. The adhesion energy can be defined as the energy spent by the cell when its boundary sticks to an adjacent structure. In general, intra-cellular and extra-cellular forces control cell movement. Adhesion forces are acting at the interface of a cell with another biological structure touching it. This entity can either be another cell, or can be the surrounding medium. In both cases the forces acting at the interface between the two biological surfaces bound to each other are adhesive forces. The cell can either touch another cell if it is positioned inside the notochord, or it can touch the somites (lying outside the notochord) if the cell is located at the lateral edge of the notochord. Adhesion molecules are cadherin molecules expressed by the cell membrane during these interactions. Inside the cell, the polymerized cytoskeleton maintains the convex shape of the cell boundary. Cortical tension is the intra-cellular tension force acting on the cell membrane and restraining cell deformations. The cortical tension energy is the energy released by tension forces exerted by the cortex microfilaments interacting with the cell membrane. Cortical tension molecules are the molecules involved in the contractility of the cortex filaments such as actomyosin [12]. Thus, the model accounts for two different types of cell contacts: cell-to-cell and cell-to-wall; both resulting in surface tension variations. Note that the cell-to-medium contact is neglected here since the experimental observations reveal very limited space between cells. It is a general belief that cell intercalation is the main factor contributing to the notochord formation. The goal of this paper is to find an explanation of a rather general problem: how the mechanical properties of cells at the boundaries, particularly adhesion and cortical tension, contribute to intercalation or large scale remodeling of tissues seen during embryonic development. We examine the role of differentially distributed surface tension (anisotropic adhesion and cortical tension) as a possible cause of notochord convergent extension (through cellular intercalation); particularly, we investigate whether anisotropic adhesion and cortical tension can serve as the main driving mechanism responsible for intercalation in zebrafish gastrulation. We also aim to test if the changes in cell behavior found in mutant embryos lacking noncanonical Wnt signaling can be explained by loss of oriented adhesive function. To examine the effects of loss of adhesion on this system, we use embryos mutant for the adhesion molecule E-Cadherin, which mediates part of the cell-cell adhesion (similar to the molecules like Ncad and protocadherins). Embryos lacking this adhesion molecule (Babb [1], Kane [10], Warga [16], Shimuzu [15]) exhibit delayed and incomplete gastrulation tissue movements of epiboly, convergence and extension.

In vertebrates cell rearrangements during embryonic development transform a symmetrical mass of cells into an elongated body rudiment with a recognizable head. Cells at the future dorsal midline (the notochord precursor) rearrange in order to convert a short and broad block of cells into a narrow tall one. The morphogenesis of

the notochord has been extensively studied in ascidians, vertebrate amphibians and zebrafish (Jiang and Smith [7], Keller et al. [11], Glickman [4]). During this tissue morphogenesis, cells at the dorsal midline progressively elongate perpendicular to the midline axis, and intercalate between one another. The movement of a cell between its medial neighbors displaces the neighboring cells along the midline axis (see Figures 1A, 1B, and 2). Cells situated along lateral edges of the notochord touch a boundary wall formed by the cells adjacent to the notochord (somites). The notochord cells in contact with the wall continue to bleb and show membrane activity. While their medial edges remain motile, their lateral edges become inactive. Thus, the intercalation of a cell from lateral edge to midline narrows the tissue, while the perpendicular displacement of dorsal neighbors lengthens the tissue. Some aspects of this cell rearrangement are quite complicated. Clearly, there are multiple mechanisms contributing to morphogenesis, as notochord formation is only impaired in embryos mutant for the adhesion molecule E-cadherin, or N-cadherin, or the Wnt signaling pathway, which has been shown to modulate the cell surface density of E-cadherin. What is the main cause of this morphogenesis? What are the relative contributions of differential adhesion, elongation and alignment, along with chemotaxis-driven protrusion and stiffness?

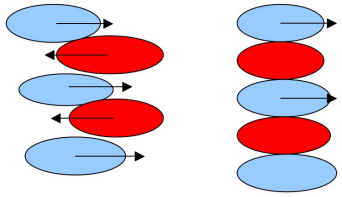

FIGURE 1. A. Cells intercalating, B. Cells ending intercalation.

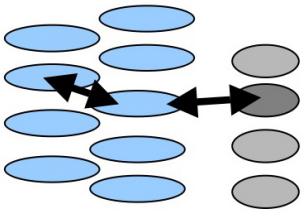

FIGURE 2. Blue Cells=Notochord Cells, Grey Cells=Somites (adjacent to notochord).

In the experiment of the zebrafish embryo during gastrulation in the notochord region cell movements are observed from time-lapse images. Cells progressively elongate, intercalate between one and another, and ultimately stack up forming a cohesive narrow rod-like structure, see Fig.1. According to our model, cellular adhesion and cortical tension are believed to be prevailing factors in this particular formation. What is the role of surface tension of cell boundaries when the

cells are in contact with each other to achieve this particular configuration? In order to understand the mechanism behind cellular intercalation, we use a simple mathematical model based on the existence of anisotropic surface tension molecules and their effect on the process of intercalation. In our model in addition to adhesion molecules (Zajac [18]), we consider the presence of cortical tension molecules unevenly distributed along each cell boundary. The existence of the competitive effect of cortex tension has been considered by a number of authors in studying the development of various species. One example is a mechanical model for the morphogenesis of the Xenopus laevis suggested by M. Weliky et al. [17]. In this model the adhesive forces are counterbalanced by tension forces at the cell junctions. The cell boundaries with no protrusive activity have been shown to have more cortex tension than their active counterparts of apparent protrusions. Similar conclusions were made by various authors in the study of Drosophila (T. Lecuit, P.F. Lenne [13], J. Kafer et al. [8] , H. Honda et al. [6]), Dictyostelium (J. Kafer, P. Hogeweg, A. Maree [9]), and zebrafish embryo (R. Grima, S. Schnell [5], M. Krieg et al. [12]). Mathematical modeling of intercalation allows one to analyze various factors contributing to the cell movement that are difficult to separate in vivo. In order to capture the essential factors responsible for convergence and extension movements (such as cellular intercalation) we use a simplified version (model) of what we believe is happening in reality. In our model we attempt to describe cellular intercalation as a collective behavior of simplified cell structures that can drive morphogenetic tissue organization. According to our model local properties of cells at the cell boundaries averaged over groups of cells and time intervals contribute to the cell rearrangements at the large tissue level. Note that in addition to the interaction of cells that are in contact with each other, chemotaxis as a global interaction can also be an important contributing factor (chemotaxis was recently shown to be a dominant effect in a model of adhesion-based cell sorting (Kafer, J. et. al. [9]). The analysis of the role of chemotaxis for the notochord development will be done elsewhere.

Let us note that experimental observations of notochord development from embryos include various data regarding the number of cells, cell outlines (elongation, orientation, perimeter, area or volume), direction of cell migration or intercalation, and the fact of non-adherence of notochord to somites. Note also that the main components of our model: anisotropic adhesion and cortical tension are not directly observed in the experiment. In our analysis, these factors are considered as variables. We examine variations of the total surface tension energy with respect to the change of these variables within their range of values for different types of cell contacts (cell-to-cell or cell-to-wall).

2. **The model.**

Our model is based on the leading role played by anisotropic surface tension (cellular adhesion and cortical tension) in the process of intercalation. The idea of an important role played by anisotropic adhesion for cell intercalation of the frog Xenopus laevis was first developed in the work of Zajac, Jones and Glazier [18]. In our model the cortical tension is defined as the surface tension caused by the contraction of the cortex microfilaments interacting with the cell boundary. Using the Cellular Potts Model (CPM) [3], we consider the cells as a group of clustered sites defined on a lattice grid. We assume that adjacent cells intercalate by sticking to each other in a particular manner, and the strength of their adhesion varies along their boundaries. As noted above, our model considers the presence of

anisotropic surface tension molecules that are unevenly distributed along each cell boundary. Each contact point on the boundary is assigned a certain energy value corresponding to its surface tension. Note that this assignment is not dictated by parameters of the model and is model dependent. There are various approaches in the literature both within CPM models [12] as well as models using other techniques, e.g. those based on differential equations [6]. The energy of each cell is calculated depending on the type of cellular contact, cell elongation, and relative orientation of the cell with respect to its neighbors. The energy values assigned to the contact (boundary) sites vary along the cell boundary, with greater values on the short sides and smaller values on the long sides of the cell [18]. The total energy of the system can be calculated by adding the energies of all cells. We verify that our cell rearrangements follow the general rule of minimization of the total energy of the system. We assume that the total energy variations depend only upon the surface tension of the cells that are in direct contact with each other and all other factors such as chemotaxis, apoptosis or division of cells are considered secondary and ignored. The calculations of our model of zebrafish embryo development are performed in both two and three dimensions using Mathematica programming; the details of our analysis are given for two-dimensional cell configurations.

2.1. **Two-dimensional model.** According to the cellular automata theory we discretize our domain with a two-dimensional grid of square lattice sites (pixels). The size of each site is determined by the resolution chosen for the picture. A finer resolution better represents the cell outline but involves more extensive computations since each cell is represented by a larger set of pixels. Experimental data from time-lapse images consist of a list of (x,y) coordinates of vertices in 2D (and (x,y,z) coordinates for 3D case) for all cells. Cell outlines are drawn for each cell and lattice sites are obtained by covering all cell outlines. Each cell is represented by an assembly of sites. The behavior of each site is determined by its interaction with the neighboring sites. This formalism is based on the Cellular Potts Model, see Glazier and Graner [3]. According to this formalism, cells cover multiple sites on the lattice and have some of the properties of real biological cells that we assume relevant to the observed behavior. In the experiment we can observe changes in cell outlines at different time intervals. Since experimentally it is difficult to separate the energies of surface adhesion and cortical tension at the cell boundaries, in our model we calculate their sum: the combined surface tension energy. Since the surface adhesion energy is determined by the cell adhesiveness, and the cortical tension energy is determined by the cell stiffness, our total energy is the function of both variables combined: adhesiveness and stiffness of the cells. The details of total energy calculation are given below.

Each cell has interior and boundary lattice sites (see Figure 7). The surface tension energy between two interior sites is 0, according to our assumption of no adhesiveness or stiffness inside the cell. The surface tension energy of a boundary lattice site at a contact point is represented by the function $Z[\sigma(r), \sigma(r_k)]$. For each boundary site of the cell the position vector $r = (x, y)$ is defined as the vector connecting the center of the cell G with the point M of its contact with an adjacent cell (see Figure 3). Each cell and all its sites (with different r) are assigned the same index $\delta = \sigma(r)$. For an adjacent cell we can introduce in a similar manner $\sigma(r_k)$ as the index value of an adjacent cell with position vector r_k at the contact site M, where $k = 1, ..., 4$ (Figure 4). All boundary sites of the adjacent cell to the north of our cell are assigned a value $k = 1$, to the east of it $k = 2$, etc. (Figure 4b). The

computer program picks one particular cell and calculates the total contribution to the surface tension energy with all its adjacent cells at all contact points. Then the program sums the contributions from all cells in the domain. The surface tension energy $Z[\sigma(r), \sigma(r_k)]$ is evaluated according to the following expression,

$$Z[\sigma(r), \sigma(r_k)] = J[\sigma(r), \sigma(r_k)] - Q[r, r_k], \tag{1}$$

where $J[\sigma(r), \sigma(r_k)] > 0$ represents the isotropic part of the surface tension energy (adhesion and cortical tension) of the two sites in contact, and $Q[r, r_k]$ is the polar term reflecting the anisotropic part of the surface tension energy, see Zajac [3]:

$$Q[r, r_k] = \alpha\alpha_k\epsilon\epsilon_k r r_k \, sin\theta \, sin\theta_k. \tag{2}$$

Note that the term $J[\sigma(r), \sigma(r_k)]$ depends only on the type of contact and is constant along the cell boundary. In our model we approximate every cell as an ellipse and by elongation vector we mean a vector along its major axis a (Figure 5). In expression (2) θ is the angle between the elongation vector v of our cell and the position vector r at the contact point M (see Figure 3). Correspondingly, θ_k is the angle between the elongation vector v_k of an adjacent cell and the position vector r_k at the contact point M.

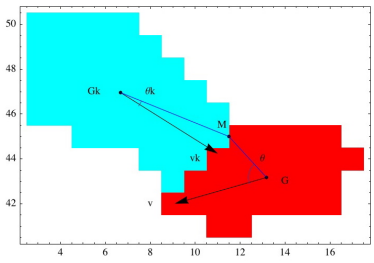

FIGURE 3. Red cell and its neighbor blue cell at the contact point M. The position vectors are $GM = r$ and $G_kM = r_k$. The cell elongation vectors are v and v_k.

From the cell outlines we can compute the total energy of the system of cells at different time intervals:

$$\begin{aligned} H &= \sum_{r\in\Omega}\sum_{k=1}^{4} k_D \left(J[\sigma(r), \sigma(r_k)] - \alpha\alpha_k\epsilon\epsilon_k r r_k \, sin\theta \, sin\theta_k\right) \\ &= \sum_{r\in\Omega}\sum_{k=1}^{4} k_D Z[\sigma(r), \sigma(r_k)], \end{aligned} \tag{3}$$

where

$$k_D = \begin{cases} 0, & \sigma(r) = \sigma(r_k) \\ 1, & \sigma(r) \neq \sigma(r_k) \end{cases}$$

and Ω is the domain of lattice sites. The case $k_D = 0$ means that the two sites of the same cell have zero surface tension. And $Z[\sigma(r), \sigma(r_k)]$ is the surface tension energy

between two lattice sites of coordinates $r = (x, y)$ and $r_k = (x_k, y_k)$ either inside the notochord between two distinct cells, or at the lateral border of the notochord between one cell at the edge and the wall. Let $\sigma(r) = \delta$, $\sigma(r_k) = \delta_k$, where δ and δ_k represent two different index values, meaning that the lattice site r and its adjacent site r_k belong to distinct boundaries of two biological contact surfaces, otherwise the terms in the first sum of (1) would all be zeros. The value of the isotropic surface energy $J[\sigma(r), \sigma(r_k)] = J(\delta, \delta_k)$ changes depending on the nature of the surfaces in contact since we have two different cellular contacts: cell-to-cell and cell-to-wall. The two-dimensional lattice site of index δ also called the center site, has a 4-point neighborhood that contains the other sites of index δ_k, $1 \leq k \leq 4$, see Figure 4. Usually in the Cellular Potts Model there is also a contribution to the total energy from the volume and surface-area constraints which in the CPM simulations prevent cells from disappearing and losing their roundness, respectively. Since this work does not simulate cell movements, the energy contribution from these CPM terms is effectively constant and it does not affect the total energy change. In our model we do not simulate cell movements but rather use cell movement experimental data to calculate total surface energy. Therefore no additional constraints are needed in equation (3).

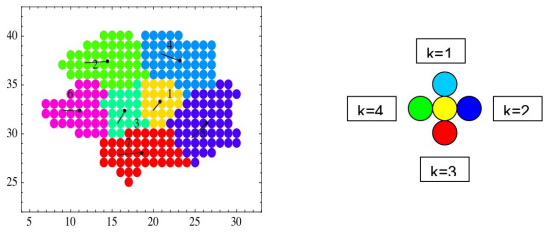

FIGURE 4. A. Cluster of 7 cells. Cell 1 is the set of yellow pixels (sites=circles). Each circle is represented by $\sigma(r) = \delta$, i.e. cell number (yellow=1, green=2). B. Center site (yellow pixel) surrounded by its four adjacent sites.

In the model we approximate every cell as an ellipse of eccentricity ϵ, and by elongation vector we mean a vector along its major axis a (cell elongation). The parameter ϵ is the cell elongation measure, $\epsilon = \sqrt{1 - (b/a)^2}$, where a is determined as the maximum distance between two opposite boundary points in the direction of the cell elongation vector and b is the minimum distance in the direction perpendicular to the elongation vector, so that b/a represents the width-to-length ratio. Cell polarity characterizes how different the cell is from the circular shape, it is related to eccentricity of the ellipse approximating the cell: if the ratio b/a is close to 1 (ϵ is close to zero) then we say that the cell is not polarized but more rounded; if b/a is close to zero (ϵ is close to 1) then the cell is very elongated and polarized.

The parameter $\alpha > 0$ (or $\alpha_k > 0$) is the weight of the polar term in its contribution to the total energy of the cell. When the angles θ and θ_k at the contact point are 90^o, the polar term is maximum, and the total energy is minimum which makes it a favorable contact for the cells. Therefore cells tend to position themselves in contact along their long sides, see Fig. 6.

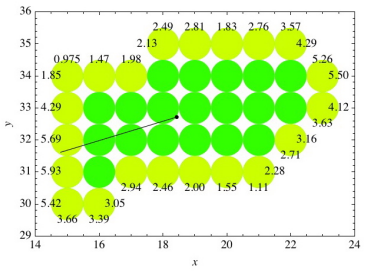

FIGURE 5. A cell approximated by an ellipse.

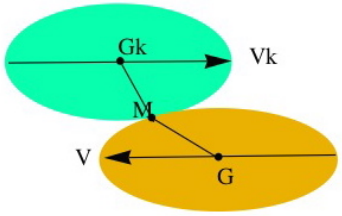

FIGURE 6. Two cells (approximated by ellipses) are in contact with each other along their longer sides.

The observations of the zebrafish embryo development in vivo during gastrulation in the notochord region provide data on cell contours for a group of notochord cells at different time points. We analyze a subset of this data, taken from the mid-region (cluster) to avoid interference with the top and bottom open boundaries where the cell outlines are not completely defined. In order to reduce the amount of data we superimpose a two-dimensional lattice over the cell outlines and choose a larger scale of resolution 8x8 where now 8x8 pixels of experimental data are represented by a 1x1 big numeric pixel (Figure 8), and similarly for a 4x4 resolution, 4x4 pixels of experimental data are represented by a 1x1 numeric pixel (Figure 9). As an example, Figure 7 presents the values of the surface tension energy calculated for one cell at its boundary contact points. The cell is located inside the notochord away from the wall, and therefore is touching other notochord cells (not shown in the figure). The x and y axes measure the width and the length of the notochord tissue, respectively. The isotropic surface tension energy J is set to 6 for cell-to-cell contacts, and the values of total anisotropic energy are calculated according to equations (1) and (2). We observed that due to the polar term Q the surface tension energy values are no longer uniformly distributed along the cell boundary sites (yellow) and reach a minimum along the longer sides of the cell.

2.2. **Three-dimensional model.** The group of cells is considered in a three-dimensional grid, where each cell is represented by a set of 3D-lattice sites. The neighborhood of a center site is expanded to six points by adding top and bottom adjacent sites. The position for each center site is represented by $r = (x, y, z)$ and its adjacent sites are located at $r_k = (x_k, y_k, z_k)$, with $1 \leq k \leq 6$. Cells are approximated by ellipsoids where center of mass and elongation vectors are calculated in

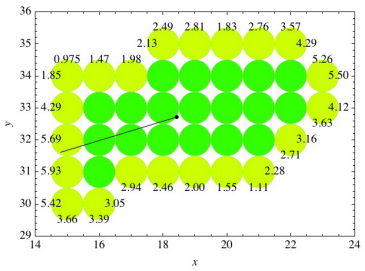

FIGURE 7. An uneven distribution of surface tension energy values for one cell inside the notochord where x measures the notochord width and y measures its length. Boundary lattice sites (yellow) are assigned energy values computed according to $Z[\sigma(r), \sigma(r_k)] = J - \alpha\alpha_k\epsilon\epsilon_k rr_k\, sin\theta\, sin\theta_k$, where $J = 6$, $\alpha = 1$, $\alpha_k = 1$, $r = (x, y)$, $14 \leq x \leq 24$, $29 \leq y \leq 36$.

three dimensions. Similar to the 2D case the total energy is computed using the equation (3).

2.3. **Computational outcomes.** Since the goal of the paper is to analyze the stability of the process of intercalation described by our model, we compute the total energy of the system of cells at 44-minute intervals. The computation of the variations of the total energy in time will show how realistic our model is. For a selected cluster of cells in the experiment we observe the changes in cell shapes at different time points. Each cell is discretized (presented as a set of lattice sites), and approximated by an ellipse. The direction of elongation vector of a cell is defined as the direction of the major axis of the corresponding ellipse and can be obtained by calculation of the cell moments of inertia about the coordinate axes, and subsequent diagonalization of the matrix of moments of inertia, see Zajac et al. [18] for details. The results of a cluster of 45 cells with cell outlines and corresponding directions of elongation are shown in Fig. 8.

2.3.1. *Effect of Surface Tension on Total Energy at Different Cell Contacts.* The analysis of the first cluster of 45 cells selected over a square lattice of 8x8 resolution is performed at three different time points (Fig.8) of 44-minute intervals. Figure 9 shows cell outlines for the second cluster of 28 cells and their direction of elongation. This second cluster is analyzed at a finer resolution 4x4 during four time points for shorter time intervals: $t_1 = 0$, $t_2 = 13$, $t_3 = 29$, $t_4 = 44$ minutes. We first observe that the direction of elongation for all cells from both Figures 8 and 9 becomes more aligned and perpendicular to the notochord axis. For both clusters we evaluate the total energy as a function of two variables, x: cell-to-cell contact energy density (energy per unit surface area per lattice site), and y: cell-to-wall contact energy density. Both variables include densities of the surface adhesion energy and cortical/cytoskeleton tension at each contact. The total surface tension energy is calculated as the sum of cell-to-cell contact energy density and cell-to-wall contact energy density over the entire square lattice. Figure 10 shows the variation of the total energy with respect to the variables x (cell-to-cell contact energy density: horizontal axis) and y (cell-to-wall contact energy density: vertical axis) from time point 1 (Tp1) to time point 3 (Tp3). Total energy values are marked with a color;

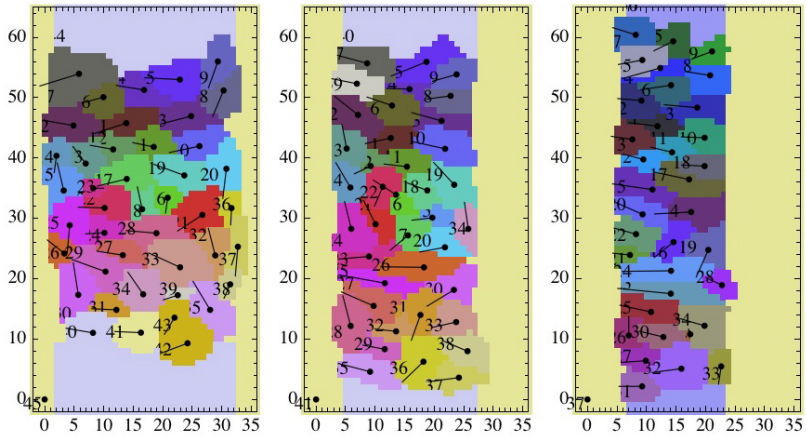

FIGURE 8. Portion of notochord showing cell outlines at three different time points (44-minute interval) over a lattice square of 8x8 resolution, where $0 \leq x \leq 35$, $0 \leq y \leq 60$. (x is the notochord width and y is the notochord length). Scale: 1 pixel= $2\mu m$.

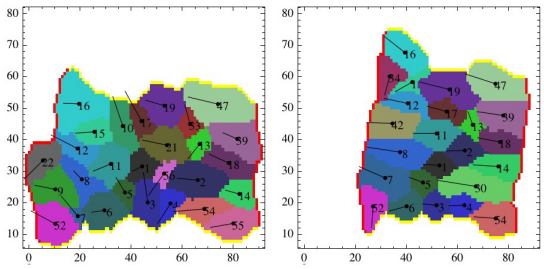

FIGURE 9. Portion of notochord (x -width, y -length) showing cell outlines from time point 1 to time point 4 (44-minute interval) over a lattice square of 4x4 resolution; $0 \leq x \leq 90$, $0 \leq y \leq 80$. Scale: 1 pixel= $1\mu m$.

light colors account for lower energies and dark colors for higher energies. On Figure 10 the energy varies from -2,300 to 20,000. A negative energy value means that the changes in the surface area of the cell resulting in the breakage of molecular bonds in the cell membrane are followed by a release of energy. We can see that the total energy is decreasing with time from Time point 1 to Time point 3; for example, at $(x, y) = (30, 30)$ the total energy reduces from black (here 20,498) to grey (here 16,824). Since the darker areas are located in the upper right corners of the window, we can conclude that higher values of total energy occur for larger energy densities (higher values of x and y) at both cell-to-cell and cell-to-wall contacts. Note that the total energy variation is more sensitive to variations in x (cell-to-cell contact energy) than in y (cell-to-wall contact energy). A negative slope of all slanted lines means that y varies in opposite direction to x for all time points when the total energy is kept constant. For example, if x decreases from 7 to 5, then in order to

keep the same value of the total energy (0) y should increase from -10 to -5. This difference in behavior of x and y suggests that different factors contribute to the total energy at cell-to-wall interface compared to cell-to-cell interface. Note that at the cell-to-wall boundary the contribution of the cortical tension to the total energy is greater than that of the adhesion; while inside the cell the contribution of adhesion prevails according to experimental observations. The case where the surface tension is zero means that there are no tension forces exerted by the cortex filaments.

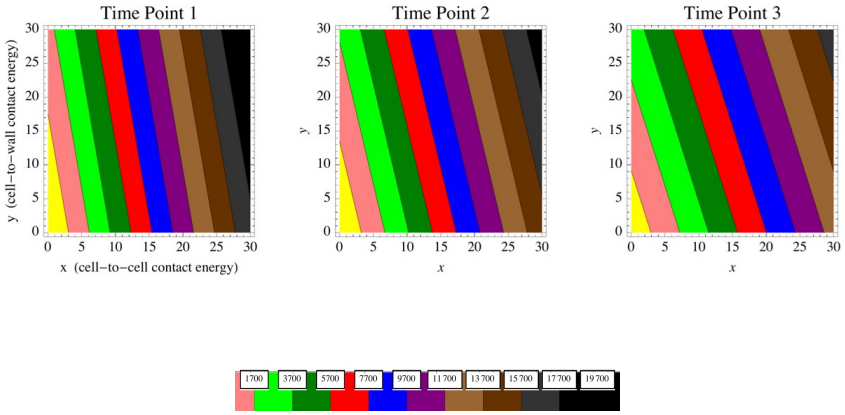

FIGURE 10. Contour plots of total energy H as a function of x and y at 3 time points of 44-minute intervals of resolution 8x8, where x is the surface cell-to-cell contact energy, and y is the surface cell-to-wall contact energy: $0 \leq x \leq 30$, $0 \leq y \leq 30$. Value of total energy H is indicated by color in color bar chart.

From both observations and calculations we see that the total number of sites covering the cluster of cells (total surface area of the cluster) decreases over time. We can also observe that the number of cells from Time point 1 to Time point 3 decreases from 43 to 35. It means that the 2D-analysis does not capture the third dimension; some cells are not seen in the two-dimensional cross-section (z-layer) of the domain because they moved to a different layer. This observation suggests the need for a 3-D analysis to more accurately account for all cells.

From our calculations we observe that the total energy evaluated at cell-to-cell contacts decreases over time, unlike the total energy at cell-to-wall contacts. With time, the cell configurations change to follow the reduction in total energy. In our model the total energy decreases with the decrease of both x and y, which represent the energy densities at the cell-to-cell and cell-to-wall contact lattice sites. Notice however, that the reduction in total energy is more significant with the decrease of x (cell-to-cell contact energy) than y (cell-to-wall contact energy). This finding tells us that the cell-to-cell contact is the prevailing contact contributing to the decrease of the total energy.

2.3.2. *Polar term and Anisotropy of Total Energy.* According to the expression (3) the dependence of the total energy polar term on the cell elongation and relative cell orientation determines the anisotropy of total energy (uneven distribution of surface tension). In our calculations we set the weight of the negative polar term

to be $\alpha = 1$. In general, α can be a function of time. For $\alpha = 1$ the absolute value of the anisotropic adhesion energy term decreases with time. Since the polar term is negative it contributes to the decrease of the total energy of the system of cells, however this negative effect is reduced over time as the magnitude of the polar term decreases from Time point 1 to Time point 3. The contribution of the polar term as time varies is of course, determined by the form of the function $\alpha = \alpha(t)$.

2.3.3. *Analysis of a Smaller Cluster.* Similar analysis has been performed for a smaller group of cells (28) during 4 time points with resolution 4x4 see Fig. 11.

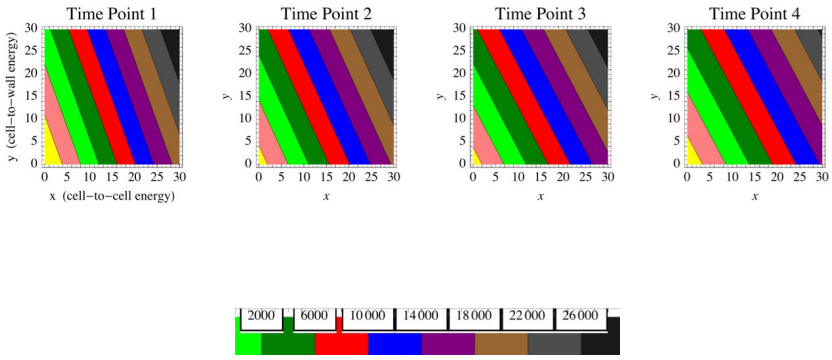

FIGURE 11. Contour plots of the total energy of the system at four different time points: $t_1 = 0$, $t_2 = 13$, $t_3 = 29$, $t_4 = 44$ minutes, for 4x4 resolution. x is the surface cell-to-cell contact energy, y is the surface cell-to-wall contact energy: $0 \leq x \leq 30$, $0 \leq y \leq 30$. The value of the total energy H is indicated by color in color bar chart.

As in the previous case with 8x8 resolution, we observe that the energy related to cell-to-cell contact decreases over time while the energy of the cell-to-wall contact in general, increases with time. The total energy of the system is decreasing function of time and the decrease is more significant for large x- and small y-values. Similar to the previous case, polar term here decreases with time from point 1 to point 4. As in the case of 8x8 resolution, the total number of cells in the cluster decreases with time.

2.3.4. *Three Dimensional Analysis.* Three dimensional analysis is performed using the same experiments as in the previous 2D case. For the 3-D case data of cell outlines at different z layers are collected at four time intervals. For each horizontal cross-section of the notochord at a particular z-level (z represents the thickness of notochord), we calculate the total number of sites covering all cell outlines of the corresponding 2D-layers at each time interval (color). This number is not constant and is represented graphically in Figure 12 by the horizontal width (x value); as we can see this value changes along the vertical direction (z). This observation justifies a need for 3-D analysis.

Notice that on Fig. 12 the number of sites decreases with time, meaning that the notochord becomes narrower and thicker. The advantage of the 3-D analysis is that it takes into account all the cells in the domain, and does not have any invisible cells as in the 2-D picture. Similar to the 2-D case in 3-dimensions we observe the

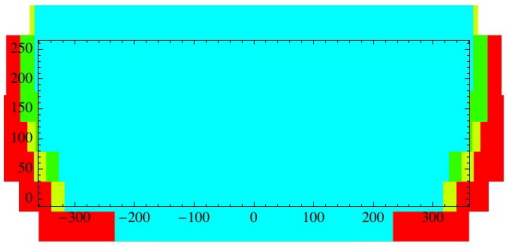

FIGURE 12. 3-D representation of total number of sites where z=const is the level corresponding to a 2-D layer of cells, and x=0 is the midline axis (notochord). Time point 1 is shown in red, Time point 2 in yellow, Time point 3 in green, Time point 4 in blue.

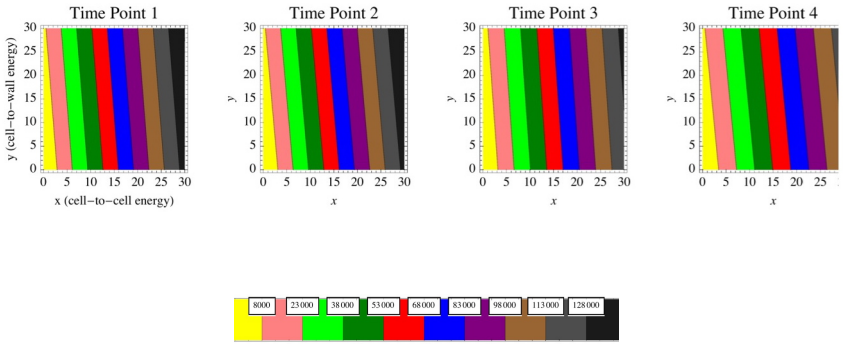

FIGURE 13. Contour plots of the 3D-total energy H(x,y) of the system at four different time points: $t_1 = 0$, $t_2 = 13$, $t_3 = 29$, $t_4 = 44$ minutes, for 8x8x5 resolution. x is the surface cell-to-cell contact energy, y is the surface cell-to-wall contact energy: $0 \leq x \leq 30$, $0 \leq y \leq 30$. The value of the total energy H is indicated by color in color bar chart.

decrease of the total energy over time (see Fig. 13), again confirming the viability of our model.

Figure 14 shows the cell outlines for the time points: $t_1 = 0$, $t_2 = 13$, $t_3 = 29$, $t_4 = 44$ minutes, at resolution 8x8x5. Similar analysis can be performed for mutant embryo with impaired E-cadherin function, see Fig. 15. We expect the cells to loose their ability to adhere effectively to each other. We observe that the notochord does not narrow or elongate properly (as for the non-mutant case). We compute the total energy between time point 1 and time point 4 and compare with our previous results obtained from wild type embryos. The total energy here also decreases over time, although the decrease is less significant than in the case of normal cells. In addition we observe that the total number of sites over time at the cell-to-wall contact stays almost the same, which can explain the improper elongation of the notochord and therefore impaired extension movement.

3. **Conclusion.** We have observed that the total energy of the system decreases over time. We have also noticed from the total energy point of view that cell-to-cell contacts have a greater influence on the total energy calculation than the cell-to-wall interface. The reason behind this observation is the fact that the number of sites contributing to cell-to-cell interaction is considerably greater than the number of cell-to-wall contact sites. Therefore cell-to-cell contacts have a greater effect on the energy decrease and on cell system stability than the cell-to-wall contacts. Both 2D and 3D studies show a decrease of the total energy with time, mainly due to the reduction of cell-to-cell contact energy. We conclude therefore, that the cell configuration changes are mainly determined by the cell-to-cell interactions rather than cell-to-wall contacts. Experimental observations show that cell boundaries at the wall remain inactive showing no signs of protrusion, and cell boundaries inside the notochord experience extensive protrusive activity. These facts suggest that cortical tension would be prevailing factor at the wall while adhesion would become an important factor inside the notochord at the cell-to-cell contacts. Despite the fact that we could not separate the adhesion energy from the cortical tension energy, our analysis (computation of total energy) shows that the variations in energy at the cell-to-wall interface are opposite to the variations in energy at the cell-to-cell contacts. This fact is in agreement with the idea that adhesion and cortical tension at the cell boundary balance each other out. Opposite situation occurs at the cell-to-cell interface with prevailing role of adhesion energy inside the domain compare to the cell-to-wall interface with prevailing cortical tension effect.

We have formulated a mathematical model describing a notochord formation due to cell intercalation and cell motion. The main consideration in our model was given to the mechanism of cellular intercalation as a result of anisotropic cellular surface tension. The total energy computed from real data at 3 time points of resolution 8x8, and at 4 different time points of resolution 4x4 decreases with time. This is a positive indication that our model can be a true approximation of what happens in reality, and anisotropic adhesion and cortical tension at cell-to-cell and cell-to-wall contacts could serve as the main driving mechanism for intercalation in zebrafish gastrulation. We concentrated on the modeling of zebrafish notochord embryo formation due to availability of experimental data and simplicity of the structure. The model however, can be applied to more general developmental biological structures.

Possible future development:

i) Analysis of other factors contributing to the intercalation of cells. Understanding of the nature of chemotaxis effect.
ii) The effect of the open top and bottom domain boundary.
iii) Simulation of the cellular behavior, numerical outcomes and comparison with experimental data.

Acknowledgments. We thank Dr. Lilianna Solnica-Krezel and Dr. Vladimir Rosenhaus for their support and encouragement. We are also grateful to anonymous Referees for a number of useful suggestions. This work was partially supported by NIH/NIGMS grant GM-055101.

REFERENCES

[1] S. G. Babb and J. A. Marrs, *E-cadherin regulates cell movements and tissue formation in early zebrafish embryos*, Dev. Dyn., **230** (2004), 263–267.

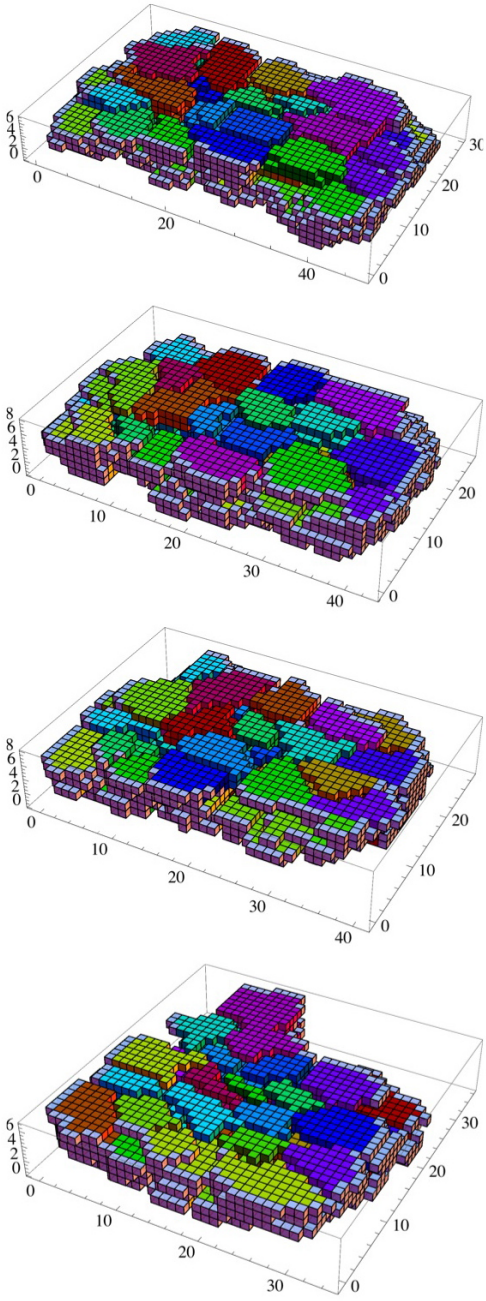

FIGURE 14. 3D-portion of notochord showing cell outlines (x: notochord width, y: length, z: thickness) at four time points: $t_1 = 0$, $t_2 = 13$, $t_3 = 29$, $t_4 = 44$ minutes, of resolution 8x8x5, where $0 \leq x \leq 40$, $0 \leq y \leq 40$, $0 \leq z \leq 6$. Scale in x and y-axes: 1 pixel $= 2\mu m$, scale in z-axis: $1.22\mu m$.

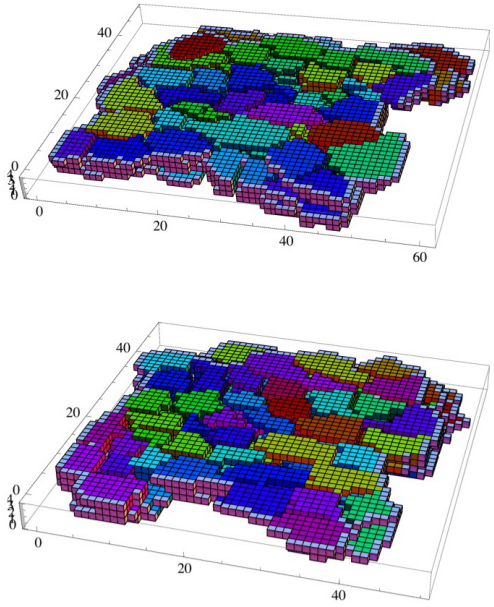

FIGURE 15. 3D-portion of notochord showing cell outlines (x: notochord width, y: length, z: thickness) from mutant embryo with E-cadherin deficiency at time point 1 and time point 4 (95 minute interval) of resolution 8x8x6, where $0 \leq x \leq 60$, $0 \leq y \leq 50$, $0 \leq z \leq 4$. Scale in x and y-axes: 1pixel $= 2\mu m$, scale in z-axis: $1.5\mu m$.

[2] T. M. Backes, R. Latterman, S. A. Small, S. Mattis, G. Pauley, E. Reilly and S. R. Lubkin, *Convergent extension by intercalation without mediolaterally fixed cell motion*, J. Theor. Bio., **256** (2009), 180–186.
[3] J. A. Glazier and F. Graner, *Simulation of differential driven adhesion rearrangement of biological cells*, Phys. Rev. E., **47** (1993), 2128–2154.
[4] N. S. Glickman, *Shaping the zebrafish notochord*, Development, **130** (2003), 873–887.
[5] R. Grima and S. Schnell, *Can tissue surface tension drive somite formation?*, Develop. Biol., **307** (2007), 248–257.
[6] H. Honda, T. Nagai and M. Tanemura, *Two different mechanisms of planar cell intercalation leading to tissue elongation*, Develop. Dyn., **237** (2008), 1826–1836.
[7] D. Jiang and WC. Smith, *Ascidian notochord morphogenesis*, Develop. Dyn., **236** (2007), 1748–1757.
[8] J. Kafer, T. Hayashi, A. F. Mare, R. W. Carthew and F. Graner, *Cell adhesion and cortex contractility determine cell patterning in the Drosophila retina*, Proc. Natl. Acad. Sci., **104** (2007), 18549–18554. arXiv:0705.1057
[9] J. Kafer, P. Hogeweg and A. F. Maree, *Moving forward backward:directional sorting of chemotactic cells due to size and adhesion differences*, Comput. Biol., **2** (2006), 518–529.
[10] D. A. Kane, K. N. McFarland and R. M. Warga, *Mutations in half baked/E-cadherin block cell behaviors that are necessary for teleost epiboly*, Development, **132** (2005), 1105–1116.
[11] R. Keller, L. Davidson, A. Edlund, T. Elul, M. Ezin, D. Shook and P. Skoglund, *Mechanisms of convergence and extension by cell intercalation*, Philos. Trans. R. Soc. Lond B. Biol. Sci., **355** (2000), 897–922.

[12] M. Krieg, Y. Arboleda-Estudillo, P-H. Puech, J. Kafer, F. Graner, D. J. Muller and C-P. Heisenberg, *Tensile forces govern germ-layer organization in zebrafish*, Nature Cell Biol., **10** (2008), 429–436.

[13] T. Lecuit and P. Lenne, *Cell surface mechanics and the control of cell shape, tissue patterns and morphogenesis*, Nature Reviews, Molecular Cell Biology, **8** (2007), 633–644.

[14] D. Sepich, C. Calmelet, M. Kiskowski and L. Solnica-Krezel, *Initiation of convergence and extension movements of lateral mesoderm during zebrafish gastrulation*, Develop. Dyn., **234** (2005), 279–292.

[15] T. Shimizu, T. Yabe, O. Muraoka, S. Yonemura, S. Aramaki, K. Hatta, Y. K. Bae, H. Nojima H and M. Hibi, *E-cadherin is required for gastrulation cell movements in zebrafish*, Mech. Dev., **122** (2005), 747–763.

[16] RM. Warga and DA. Kane, *A role for N-cadherin in mesodermal morphogenesis in gastrulation*, Dev Biol., **310** (2007), 211–225.

[17] M. Weliky, S. Minsuk, R. Keller and G. Oster, *Notochord morphogenesis in Xenopus laevis: Simulation of cell behavior underlying tissue convergence and extension*, Develop., **113** (1991), 1231–1244.

[18] M. Zajac, G. L. Jones and J. A. Glazier, *Simulating convergent extension of anisotropic differential adhesion*, J. Theor. Bio., **222** (2003), 247–259.

Received July 25, 2009; Accepted November 26, 2009.

E-mail address: ccalmelet@csuchico.edu
E-mail address: diane.s.sepich@vanderbilt.edu